This paper appears in IET Control Theory & Applications, 2018.
http://digital-library.theiet.org/content/journals/10.1049/iet-cta.2017.1253

Impedance Control of Nonlinear Multi-DOF Teleoperation Systems with Time Delay: Absolute Stability

Mojtaba Sharifi [1,2], Hassan Salarieh [2], Saeed Behzadipour [2], Mahdi Tavakoli [1*]

[1] Department of Electrical and Computer Engineering, University of Alberta, Edmonton, Canada
[2] Department of Mechanical Engineering, Sharif University of Technology, Tehran, Iran
[*] mahdi.tavakoli@ualberta.ca

Abstract: A nonlinear robust adaptive bilateral impedance controller is proposed to provide the absolute stability of multi-DOF teleoperation systems with communication delays, in addition to the force and position tracking performance. The proposed controller realizes two desired (or reference) impedance models for the master and slave robots using a new nonlinear robust version of the Model Reference Adaptive Control (MRAC) scheme. Using the absolute stability criterion, the robustness condition of the teleoperation system against communication delays is obtained, resulting in suitable adjustments of parameter values in the desired impedance models. In addition, using the Lyapunov stability theorem, the tracking performance of the master and slave robots and the robustness of the proposed controller against parametric and bounded unstructured modeling (non-parametric) uncertainties are proven. The performance of the proposed nonlinear bilateral controller is investigated by performing some experiments on nonlinear multi-DOF telerobots with and without communication delays.

1. Introduction

In recent years, teleoperation systems have been widely used in many applications such as minimally invasive telesurgery [1, 2], telerehabilitation [3, 4] and telesonography [5]. Different control methods have been suggested for (1-DOF) linear teleoperation systems [1, 6-10]. Among them, the 4-channel control architecture is one of the most successful that provides transparency [1]; however, this control strategy requires the exact mathematical models of the master and the slave robots.

In practical settings, multi-DOF nonlinear robotic systems must be utilized instead of one-DOF linear ones. Accordingly, adaptive controllers [11, 12] have been developed for nonlinear master and slave dynamics assuming linear operator and environment dynamics. To synchronize the positions of robots with a communication delay, PD [13], adaptive [14, 15] and feedback linearization-based [16] controllers have been proposed.

To achieve both of the position and force tracking performances (transparency) in a multi-DOF system, Ryu and Kwon [17] have developed a nonlinear adaptive controller, which was modified by Liu and Tavakoli [18]. A disturbance observer-based bilateral control method has been presented in [19], which could provide transparency condition in the presence of slow-varying disturbances. Moreover, Hashemzadeh et al. [20] have recently suggested a PD control law together with gravity compensation for multi-DOF teleoperation system subjected to time delays.

Recently, some advanced robust/adaptive controllers have been developed for the position and force control of bilateral and multilateral teleoperation systems. For instance, a new wave-variable-based nonlinear adaptive control strategy with four channels has been designed in [21, 22] to improve the system transparency. The wave variables have been combined with neural networks in [23] to compensate for the effects of delays and system uncertainties. In order to have a finite-time position synchronization performance, the terminal sliding mode (TSM) control approach has been extended in [24] for bilateral teleoperation systems having constraints on the position error. In another work [25], a switching robust control method has been suggested to use multiple robust control laws scheduled based on estimation of the environment stiffness. Similarly, an adaptive robust multilateral controller has been presented in [26], where the interaction force of environment should be estimated. However, designing the controller structure based on an estimation from the environment dynamics may be challenging due to the fast variation and/or non-deterministic behaviour of some environments.

Using the impedance/admittance control theory [27-30], some interactive tasks, which cannot be performed well by pure position or force control, can be executed by a single robot. The impedance control of linear 1-DOF bilateral teleoperation systems has been employed in [31-33].

In the present work, a new nonlinear Bilateral Model Reference Adaptive Impedance Controller (BMRAIC) is developed that has the following novel characteristics:

1) Instead of previous nonlinear bilateral controllers with position and force tracking control laws, the impedance (virtual dynamics) of the teleoperation system is controlled in this study by enforcing two reference impedance models for the master and slave robots. This strategy causes that one control objective (impedance adjustment) is pursued for each of master and slave robots. However, two objectives (position and force tracking) were followed simultaneously for each robot in previous works, which were hard to be achieved.

2) While the dynamics of multi-DOF teleoperation system and the structure of the proposed controller are nonlinear, the absolute stability of the two-port teleoperation system in the presence of bounded time delays is proven. Also, the

convergence of the master and slave trajectories to their desired impedance model responses is proven in a Lyapunov framework. Note that in the previous bilateral position and force tracking controllers [17, 18, 34] for nonlinear systems, only the tracking error convergence to zero was proven and the absolute stability was not guaranteed in the presence of communication delays. It should be mentioned that the absolute stability of a two-port network guarantees the stability of the coupled system connected to two passive terminations [35]. This stability criterion can show the instability of the whole teleoperation systems due to the bilateral communication delays between its two ports.

3) Some guidelines and admissible ranges are obtained for choosing the parameters of the two impedance models from the absolute stability analysis such that the closed-loop system stability becomes robust against time delays.

4) The proposed bilateral controller is robust against parametric (structured) uncertainties of the system (via employing adaptation laws) and bounded non-parametric (unstructured) uncertainties (using robust terms).

In the previous nonlinear bilateral adaptive controllers (such as those in [17, 18]), force tracking was achieved only when the estimation of nonlinear dynamic parameters converged to the real values (persistent excitation conditions). However, both of position and force tracking goals can be obtained simultaneously in this paper without any requirement on the system parameter identification.

As a result of employing the proposed bilateral impedance controller, a trade-off between the absolute stability and transparency of the teleoperation system is obtained when communication channels have time delays. Accordingly, the performed experiments show that the appropriate transparency is achieved in the absence of time delays; however, this transparency is attenuated in the presence of delays due to the specific impedance adjustment required for the absolute stability.

2. Nonlinear Dynamic Model of a Multi-DOF Teleoperation System

The nonlinear model of an *n*-DOF teleoperation system (master and slave robots) with parametric (structured) and non-parametric (unstructured) uncertainties is expressed in the joint space as [36]:

$$\mathbf{M}_{\mathbf{q},m}(\mathbf{q}_m)\ddot{\mathbf{q}}_m + \mathbf{C}_{\mathbf{q},m}(\mathbf{q}_m,\dot{\mathbf{q}}_m)\dot{\mathbf{q}}_m + \mathbf{G}_{\mathbf{q},m}(\mathbf{q}_m) + \mathbf{F}_{\mathbf{q},m}(\dot{\mathbf{q}}_m) = \boldsymbol{\tau}_m + \boldsymbol{\tau}_h + \mathbf{d}_{\mathbf{q},m} \quad (1)$$

$$\mathbf{M}_{\mathbf{q},s}(\mathbf{q}_s)\ddot{\mathbf{q}}_s + \mathbf{C}_{\mathbf{q},s}(\mathbf{q}_s,\dot{\mathbf{q}}_s)\dot{\mathbf{q}}_s + \mathbf{G}_{\mathbf{q},s}(\mathbf{q}_s) + \mathbf{F}_{\mathbf{q},s}(\dot{\mathbf{q}}_s) = \boldsymbol{\tau}_s - \boldsymbol{\tau}_e + \mathbf{d}_{\mathbf{q},s} \quad (2)$$

where $\mathbf{q}_m$ and $\mathbf{q}_s \in \mathbb{R}^{n\times 1}$ are the joint positions, $\mathbf{M}_{\mathbf{q},m}(\mathbf{q}_m)$ and $\mathbf{M}_{\mathbf{q},s}(\mathbf{q}_s) \in \mathbb{R}^{n\times n}$ are the inertia matrices, $\mathbf{C}_{\mathbf{q},m}(\mathbf{q}_m,\dot{\mathbf{q}}_m)$ and $\mathbf{C}_{\mathbf{q},s}(\mathbf{q}_s,\dot{\mathbf{q}}_s) \in \mathbb{R}^{n\times n}$ represent the Coriolis and centrifugal terms, $\mathbf{G}_{\mathbf{q},m}(\mathbf{q}_m)$ and $\mathbf{G}_{\mathbf{q},s}(\mathbf{q}_s) \in \mathbb{R}^{n\times 1}$ are the gravity terms, $\mathbf{F}_{\mathbf{q},m}(\dot{\mathbf{q}}_m)$ and $\mathbf{F}_{\mathbf{q},s}(\dot{\mathbf{q}}_s) \in \mathbb{R}^{n\times 1}$ are the friction torques, and $\boldsymbol{\tau}_m$ and $\boldsymbol{\tau}_s \in \mathbb{R}^{n\times 1}$ are the vectors of the control torques for the master and the slave robots, respectively. Also, $\boldsymbol{\tau}_h$ and $\boldsymbol{\tau}_e \in \mathbb{R}^{n\times 1}$ are the external torques that the human operator applies to the master robot and the slave robot applies to the environment, respectively. The vectors of bounded (non-parametric) unstructured modeling uncertainties and/or bounded exogenous disturbances in the system are denoted by $\mathbf{d}_{\mathbf{q},m}$ and $\mathbf{d}_{\mathbf{q},s}$ for the master and the slave, respectively. Then, the robots end-effectors' equations of motion in the Cartesian space are expressed as

$$\mathbf{M}_{\mathbf{x},m}(\mathbf{q}_m)\ddot{\mathbf{x}}_m + \mathbf{C}_{\mathbf{x},m}(\mathbf{q}_m,\dot{\mathbf{q}}_m)\dot{\mathbf{x}}_m + \mathbf{G}_{\mathbf{x},m}(\mathbf{q}_m) + \mathbf{F}_{\mathbf{x},m}(\dot{\mathbf{q}}_m) = \mathbf{f}_m + \mathbf{f}_h + \mathbf{d}_{\mathbf{x},m} \quad (3)$$

$$\mathbf{M}_{\mathbf{x},s}(\mathbf{q}_s)\ddot{\mathbf{x}}_s + \mathbf{C}_{\mathbf{x},s}(\mathbf{q}_s,\dot{\mathbf{q}}_s)\dot{\mathbf{x}}_s + \mathbf{G}_{\mathbf{x},s}(\mathbf{q}_s) + \mathbf{F}_{\mathbf{x},s}(\dot{\mathbf{q}}_s) = \mathbf{f}_s - \mathbf{f}_e + \mathbf{d}_{\mathbf{x},s} \quad (4)$$

where $\mathbf{x}_m$ and $\mathbf{x}_s \in \mathbb{R}^{p\times 1}$ are the Cartesian coordinates of the master and slave robots' end-effectors, respectively. $\mathbf{f}_h$ and $\mathbf{f}_e \in \mathbb{R}^{p\times 1}$ are the external interaction forces that the operator applies to the master robot and the slave robot applies to the environment, respectively. $\mathbf{d}_{\mathbf{x},m}$ and $\mathbf{d}_{\mathbf{x},s}$ are also the bounded non-parametric modeling uncertainties and/or disturbances in the Cartesian space representation (3) and (4). Note that since the master and slave robots are considered to be non-redundant, the number of Cartesian coordinates (elements of $\mathbf{x}_i \in \mathbb{R}^{p\times 1}$) is the same as the number of the joint variables (elements of $\mathbf{q}_i \in \mathbb{R}^{n\times 1}$), i.e., $p = n$. Using the subscript $i = m$ for the master and $i = s$ for the slave, the relations between the matrices of dynamic models in the joint space ((1) and (2)) and the Cartesian space ((3) and (4)) with non-singular Jacobian matrices $\mathbf{J}_i(\mathbf{q}_i)$ are:

$$\begin{aligned} &\mathbf{M}_{\mathbf{x},i} = \mathbf{J}_i^{-T}\mathbf{M}_{\mathbf{q},i}\,\mathbf{J}_i^{-1},\ \mathbf{C}_{\mathbf{x},i} = \mathbf{J}_i^{-T}\left(\mathbf{C}_{\mathbf{q},i} - \mathbf{M}_{\mathbf{q},i}\mathbf{J}_i^{-1}\dot{\mathbf{J}}_i\right)\mathbf{J}_i^{-1} \\ &\mathbf{G}_{\mathbf{x},i} = \mathbf{J}_i^{-T}\mathbf{G}_{\mathbf{q},i},\ \mathbf{F}_{\mathbf{x},i} = \mathbf{J}_i^{-T}\mathbf{F}_{\mathbf{q},i},\ \mathbf{d}_{\mathbf{x},i} = \mathbf{J}_i^{-T}\mathbf{d}_{\mathbf{q},i} \\ &\mathbf{f}_i = \mathbf{J}_i^{-T}\boldsymbol{\tau}_i,\ \mathbf{f}_h = \mathbf{J}_m^{-T}\boldsymbol{\tau}_h,\ \mathbf{f}_e = \mathbf{J}_s^{-T}\boldsymbol{\tau}_e \end{aligned} \quad (5)$$

with the following properties [34, 36, 37]:

Property 1. $\mathbf{M}_{\mathbf{x},i}(\mathbf{q}_i)$ *is symmetric and positive definite.*

Property 2. $\left(\dot{\mathbf{M}}_{\mathbf{x},i}(\mathbf{q}_i) - 2\mathbf{C}_{\mathbf{x},i}(\mathbf{q}_i,\dot{\mathbf{q}}_i)\right)$ *is skew symmetric.*

Property 3. *The left side of (1) and (2) can be linearly parameterized as*

$$\mathbf{M}_{\mathbf{q},i}(\mathbf{q}_i)\boldsymbol{\varphi}_{\mathbf{1},i} + \mathbf{C}_{\mathbf{q},i}(\mathbf{q}_i,\dot{\mathbf{q}}_i)\boldsymbol{\varphi}_{\mathbf{2},i} + \mathbf{G}_{\mathbf{q},i}(\mathbf{q}_i) + \mathbf{F}_{\mathbf{q},i}(\dot{\mathbf{q}}_i) = \mathbf{Y}_{\mathbf{q},i}(\boldsymbol{\varphi}_{\mathbf{1},i},\boldsymbol{\varphi}_{\mathbf{2},i},\mathbf{q}_i,\dot{\mathbf{q}}_i)\boldsymbol{\alpha}_{\mathbf{q},i} \quad (6)$$

where $\boldsymbol{\alpha}_{\mathbf{q},i}$ is the vector of unknown parameters of the robot. The regressor matrix $\mathbf{Y}_{\mathbf{q},i}$ contains known functions [36] in terms of the vectors $\boldsymbol{\varphi}_{\mathbf{1},i}$ and $\boldsymbol{\varphi}_{\mathbf{2},i}$.

The main problem considered in this work is nonlinear impedance control of master and slave robots

(modelled in Eqs. (3) and (4)) such that position synchronization and force reflection are achieved; however, one control objective is pursued for each robot. Moreover, the absolute stability of the whole teleoperation system is provided in the presence of communication delays by adjustment of the impedance models.

3. Nonlinear Robust Adaptive Bilateral Impedance Control

An overview of the teleoperation system including the communication channels with bounded delays of T_1 and T_2 are illustrated in Fig. 1. The input and output signals of the communication channels are related as

$$\begin{aligned} &\mathbf{x}_m^d(t)=\mathbf{x}_m(t-T_1), \quad \dot{\mathbf{x}}_m^d(t)=\dot{\mathbf{x}}_m(t-T_1) \\ &\mathbf{f}_h^d(t)=\mathbf{f}_h(t-T_1), \qquad \mathbf{f}_e^d(t)=\mathbf{f}_e(t-T_2) \end{aligned} \quad (7)$$

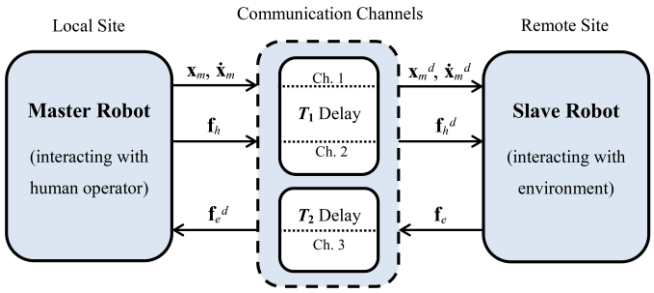

Fig. 1. *The transmission of signals using delayed communication channels.*

3.1. Desired Reference Impedance Models of Master and Slave

The reference impedance model of the master is defined as

$$m_m\ddot{\mathbf{x}}_{\mathrm{mod}_m}+c_m\dot{\mathbf{x}}_{\mathrm{mod}_m}=\mathbf{f}_h-k_{\mathrm{f}}\,\mathbf{f}_e^d \quad (8)$$

where $\mathbf{x}_{\mathrm{mod}_m}$ is the response (position) of the master reference impedance model. The measured generalized interaction forces $\mathbf{f}_h$ and $\mathbf{f}_e^d$ are the inputs of the master impedance model (8), and k_{f} is the force scaling factor. Also, m_m and c_m are the desired virtual mass and damping coefficients of the master reference (impedance) model, respectively.

The reference impedance model of the slave is expressed as

$$m_{\mathrm{s}}\ddot{\tilde{\mathbf{x}}}_{\mathrm{mod}_s}+c_{\mathrm{s}}\dot{\tilde{\mathbf{x}}}_{\mathrm{mod}_s}+k_{\mathrm{s}}\tilde{\mathbf{x}}_{\mathrm{mod}_s}=-\mathbf{f}_e \quad (9)$$

where $\tilde{\mathbf{x}}_{\mathrm{mod}_s}=\mathbf{x}_{\mathrm{mod}_s}-k_{\mathrm{p}}\,\mathbf{x}_m^d$ is the error of the slave reference impedance model's response with respect to the scaled master position and k_{p} is the position scaling factor. m_s, c_s and k_s are the desired virtual mass, damping, and stiffness coefficients of the slave reference (impedance) model. It should be mentioned that using Eq. (9), the acceleration ($\ddot{\mathbf{x}}_m^d$) of master robot is required to obtain the desired slave reference model acceleration ($\ddot{\mathbf{x}}_{\mathrm{mod}_s}$). Since the measurement of the master robot acceleration ($\ddot{\mathbf{x}}_m^d$) is prone to noise, it is estimated from Eq. (8) considering T_1 as the time delay for all signals:

$$\hat{\ddot{\mathbf{x}}}_m^d=m_m^{-1}\left(\mathbf{f}_h^d-k_{\mathrm{f}}\mathbf{f}_e^{dd}\right)-m_m^{-1}c_m\,\dot{\mathbf{x}}_{\mathrm{mod}_m}^d \quad (10)$$

where $\mathbf{f}_e^{dd}(t)=\mathbf{f}_e^d(t-T_1)=\mathbf{f}_e(t-T_1-T_2)$ has T_1+T_2 time delay.

The proposed bilateral impedance control strategy can satisfy the position tracking and force reflection goals by an adjustment of the parameters in two reference impedance models (9) and (8), respectively. In the master reference model (8), the human operator can control smoothly the desired position, velocity and acceleration ($\mathbf{x}_{\mathrm{mod}_m}$, $\dot{\mathbf{x}}_{\mathrm{mod}_m}$ and $\ddot{\mathbf{x}}_{\mathrm{mod}_m}$) that are tracked by the master robot via applying his appropriate force $\mathbf{f}_h$ on this robot. Since the generated master acceleration and velocity ($\ddot{\mathbf{x}}_{\mathrm{mod}_m}$ and $\dot{\mathbf{x}}_{\mathrm{mod}_m}$) are not too large in common operations, the left side of (8) becomes small by choosing sufficiently small values for the impedance parameters m_m and c_m. Accordingly, the right side of (8) should also be small ($(\mathbf{f}_h-k_{\mathrm{f}}\,\mathbf{f}_e^d)\to 0$); thus, the force reflection performance is achieved. However, if the human operator or the environment applies sudden large forces ($\mathbf{f}_h$ or $-\mathbf{f}_e^d$) that generate large desired acceleration and velocity ($\ddot{\mathbf{x}}_{\mathrm{mod}_m}$ and $\dot{\mathbf{x}}_{\mathrm{mod}_m}$), the force tracking error $(\mathbf{f}_h-k_{\mathrm{f}}\,\mathbf{f}_e^d)$ at the right side of (8) increases. Since the slave-environment interaction force $-\mathbf{f}_e$ at the right side of (9) is bounded, the left side of Eq. (9) is also bounded. Consequently, employing large values for the slave impedance parameters (m_s, c_s and k_s) in the left side of (9), the tracking error $\tilde{\mathbf{x}}_{\mathrm{mod}_s}$ becomes small, and the position tracking performance ($\mathbf{x}_{\mathrm{mod}_s}\to k_{\mathrm{p}}\mathbf{x}_m^d$) is obtained.

3.2. Nonlinear Robust Adaptive Control Laws

The architecture of the proposed nonlinear bilateral impedance controller is shown in Fig. 2.

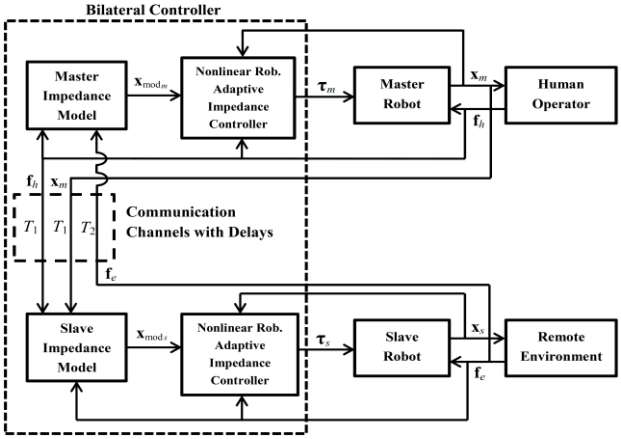

Fig. 2. *Architecture of the nonlinear bilateral impedance controller.*

The nonlinear robust adaptive control laws of the master and slave are developed according to the new nonlinear MRAIC scheme presented in [30] for one robot. The parameters of the master and slave reference impedance models (8) and (9) have the following properties:

$$\left(m_m^{-1}c_m\right)>0\ ,\ \left(m_s^{-1}c_s\right)>0\ ,\ \left(m_s^{-1}k_s\right)>0 \quad (11)$$

In the MRAIC scheme, the controller benefits from the characteristics of the reference model [30]. Thus, according to the reference impedance models dynamics (8) and (9), and using their property (11), the sliding surfaces are designed as

$$\begin{aligned}\mathbf{s}_m &= \dot{\tilde{\mathbf{x}}}_m+\left(m_m^{-1}c_m\right)\tilde{\mathbf{x}}_m+\lambda_{2,m}\int_0^t\tilde{\mathbf{x}}_m\,dt\ ,\\ \mathbf{s}_s &= \dot{\tilde{\mathbf{x}}}_s+\left(m_s^{-1}c_s\right)\tilde{\mathbf{x}}_s+\left(m_s^{-1}k_s\right)\int_0^t\tilde{\mathbf{x}}_s\,dt\end{aligned} \quad (12)$$

where $\lambda_{2,m}$ is a positive constant parameter. $\tilde{\mathbf{x}}_m=\mathbf{x}_m-\mathbf{x}_{\mathrm{mod}_m}$ and $\tilde{\mathbf{x}}_s=\mathbf{x}_s-\mathbf{x}_{\mathrm{mod}_s}$ are the master and slave position errors with respect to the responses of their impedance models (8) and (9). The reference velocities are also expressed as

$$\begin{aligned}\dot{\mathbf{x}}_{\mathbf{r},m} &= \dot{\mathbf{x}}_{\mathrm{mod}_m}-\left(m_m^{-1}c_m\right)\tilde{\mathbf{x}}_m-\lambda_{2,m}\int_0^t\tilde{\mathbf{x}}_m\,dt\\ \dot{\mathbf{x}}_{\mathbf{r},s} &= \dot{\mathbf{x}}_{\mathrm{mod}_s}-\left(m_s^{-1}c_s\right)\tilde{\mathbf{x}}_s-\left(m_s^{-1}k_s\right)\int_0^t\tilde{\mathbf{x}}_s\,dt\end{aligned} \quad (13)$$

Such that $\mathbf{s}_m=\dot{\mathbf{x}}_m-\dot{\mathbf{x}}_{\mathbf{r},m}$ and $\mathbf{s}_s=\dot{\mathbf{x}}_s-\dot{\mathbf{x}}_{\mathbf{r},s}$. Now, the nonlinear Bilateral Model Reference Adaptive Impedance Control (BMRAIC) laws are defined in Cartesian space as

$$\begin{aligned}\mathbf{f}_m &= \hat{\mathbf{M}}_{\mathbf{x},m}(\mathbf{q}_m)\begin{pmatrix}-\left(m_m^{-1}c_m\right)\dot{\mathbf{x}}_m-\lambda_{2,m}\tilde{\mathbf{x}}_m\\ +\left(m_m^{-1}\right)\left(\mathbf{f}_h-k_{\mathrm{f}}\mathbf{f}_e^{\,d}\right)-\lambda_{3,m}\mathbf{s}_m\end{pmatrix}\\ &+\hat{\mathbf{C}}_{\mathbf{x},m}(\mathbf{q}_m,\dot{\mathbf{q}}_m)\dot{\mathbf{x}}_{\mathbf{r},m}+\hat{\mathbf{G}}_{\mathbf{x},m}(\mathbf{q}_m)+\hat{\mathbf{F}}_{\mathbf{x},m}(\dot{\mathbf{q}}_m)-\mathbf{f}_h-\eta_m\,\mathrm{sgn}(\mathbf{s}_m)\end{aligned} \quad (14)$$

$$\begin{aligned}\mathbf{f}_s &= \hat{\mathbf{M}}_{\mathbf{x},s}(\mathbf{q}_s)\begin{pmatrix}k_{\mathrm{p}}\hat{\ddot{\mathbf{x}}}_m^{d}-\left(m_s^{-1}c_s\right)\left(\dot{\mathbf{x}}_s-k_{\mathrm{p}}\dot{\mathbf{x}}_m^{d}\right)\\ -\left(m_s^{-1}k_s\right)\left(\mathbf{x}_s-k_{\mathrm{p}}\mathbf{x}_m^{d}\right)\\ +\left(m_s^{-1}\right)\left(-\mathbf{f}_e\right)-\lambda_{3,s}\mathbf{s}_s\end{pmatrix}\\ &+\hat{\mathbf{C}}_{\mathbf{x},s}(\mathbf{q}_s,\dot{\mathbf{q}}_s)\dot{\mathbf{x}}_{\mathbf{r},s}+\hat{\mathbf{G}}_{\mathbf{x},s}(\mathbf{q}_s)+\hat{\mathbf{F}}_{\mathbf{x},s}(\dot{\mathbf{q}}_s)+\mathbf{f}_e-\eta_s\,\mathrm{sgn}(\mathbf{s}_s)\end{aligned} \quad (15)$$

Accent $\wedge$ denotes the estimated values of matrices, vectors and scalars. $\lambda_{3,m}$, $\lambda_{3,s}$, η_m and η_s are positive constants. The actual control inputs of the robots (applied in the joint space through motor torques) are obtained in terms of joint space matrices and vectors using (5) in (14) and (15) and Property 3:

$$\boldsymbol{\tau}_m=\mathbf{Y}_{\mathbf{q},m}\,\hat{\boldsymbol{\alpha}}_{\mathbf{q},m}-\mathbf{J}_m^T\mathbf{f}_h-\mathbf{J}_m^T\eta_m\,\mathrm{sgn}(\mathbf{s}_m) \quad (16)$$

$$\boldsymbol{\tau}_s=\mathbf{Y}_{\mathbf{q},s}\,\hat{\boldsymbol{\alpha}}_{\mathbf{q},s}+\mathbf{J}_s^T\mathbf{f}_e-\mathbf{J}_s^T\eta_s\,\mathrm{sgn}(\mathbf{s}_s) \quad (17)$$

where $\mathbf{Y}_{\mathbf{q},m}$ and $\mathbf{Y}_{\mathbf{q},s}$ are obtained from Eq. (6) in terms of the following $\boldsymbol{\varphi}_{1,m}$, $\boldsymbol{\varphi}_{1,s}$, $\boldsymbol{\varphi}_{2,m}$, and $\boldsymbol{\varphi}_{2,s}$ vectors:

$$\begin{aligned}\boldsymbol{\varphi}_{1,m} &= \mathbf{J}_m^{-1}\begin{pmatrix}-\left(m_m^{-1}c_m\right)\dot{\mathbf{x}}_m-\lambda_{2,m}\tilde{\mathbf{x}}_m\\ +\left(m_m^{-1}\right)\left(\mathbf{f}_h-k_{\mathrm{f}}\mathbf{f}_e^{\,d}\right)-\lambda_{3,m}\mathbf{s}_m\end{pmatrix}-\mathbf{J}_m^{-1}\dot{\mathbf{J}}_m\mathbf{J}_m^{-1}\dot{\mathbf{x}}_{\mathbf{r},m},\\ \boldsymbol{\varphi}_{1,s} &= \mathbf{J}_s^{-1}\begin{pmatrix}k_{\mathrm{p}}\hat{\ddot{\mathbf{x}}}_m^{d}-\left(m_s^{-1}c_s\right)\left(\dot{\mathbf{x}}_s-k_{\mathrm{p}}\dot{\mathbf{x}}_m^{d}\right)\\ -\left(m_s^{-1}k_s\right)\left(\mathbf{x}_s-k_{\mathrm{p}}\mathbf{x}_m^{d}\right)\\ +\left(m_s^{-1}\right)\left(-\mathbf{f}_e\right)-\lambda_{3,s}\mathbf{s}_s\end{pmatrix}-\mathbf{J}_s^{-1}\dot{\mathbf{J}}_s\mathbf{J}_s^{-1}\dot{\mathbf{x}}_{\mathbf{r},s},\\ \boldsymbol{\varphi}_{2,m} &= \mathbf{J}_m^{-1}\,\dot{\mathbf{x}}_{\mathbf{r},m}\ ,\qquad \boldsymbol{\varphi}_{2,s}=\mathbf{J}_s^{-1}\,\dot{\mathbf{x}}_{\mathbf{r},s}\end{aligned} \quad (18)$$

3.3. Closed-loop Dynamics of the Teleoperation System

By replacing the control laws (14) and (15) in the teleoperation system dynamics (3) and (4), one obtains:

$$\begin{aligned}\mathbf{M}_{\mathbf{x},m}\left(\ddot{\tilde{\mathbf{x}}}_m+\left(m_m^{-1}c_m\right)\dot{\tilde{\mathbf{x}}}_m+\lambda_{2,m}\tilde{\mathbf{x}}_m\right) &= -\lambda_{3,m}\mathbf{M}_{\mathbf{x},m}\,\mathbf{s}_m\\ -\mathbf{C}_{\mathbf{x},m}\mathbf{s}_m+\mathbf{J}_m^{-T}\mathbf{Y}_{\mathbf{q},m}\tilde{\boldsymbol{\alpha}}_{\mathbf{q},m}+\mathbf{d}_{\mathbf{x},m}-\eta_m\,\mathrm{sgn}(\mathbf{s}_m)\end{aligned} \quad (19)$$

$$\begin{aligned}\mathbf{M}_{\mathbf{x},s}\left(\ddot{\tilde{\mathbf{x}}}_s+\left(m_s^{-1}c_s\right)\dot{\tilde{\mathbf{x}}}_s+\left(m_s^{-1}k_s\right)\tilde{\mathbf{x}}_s\right) &= -\lambda_{3,s}\mathbf{M}_{\mathbf{x},s}\mathbf{s}_s\\ -\mathbf{C}_{\mathbf{x},s}\mathbf{s}_s+\mathbf{J}_s^{-T}\mathbf{Y}_{\mathbf{q},s}\tilde{\boldsymbol{\alpha}}_{\mathbf{q},s}+\mathbf{d}_{\mathbf{x},s}-\eta_s\,\mathrm{sgn}(\mathbf{s}_s)\\ +\mathbf{M}_{\mathbf{x},s}k_{\mathrm{p}}\left(\hat{\ddot{\mathbf{x}}}_m^{d}-\ddot{\mathbf{x}}_m^{d}\right)\end{aligned} \quad (20)$$

where $\tilde{\boldsymbol{\alpha}}_{\mathbf{q},m}=\hat{\boldsymbol{\alpha}}_{\mathbf{q},m}-\boldsymbol{\alpha}_{\mathbf{q},m}$ and $\tilde{\boldsymbol{\alpha}}_{\mathbf{q},s}=\hat{\boldsymbol{\alpha}}_{\mathbf{q},s}-\boldsymbol{\alpha}_{\mathbf{q},s}$ are the error vectors of the master and slave parameter estimations, respectively. Replacing the time derivatives of sliding surfaces (12) in the left side of (19) and (20) yields the final closed-loop dynamics of the teleoperation system:

$$\begin{aligned}\mathbf{M}_{\mathbf{x},m}\dot{\mathbf{s}}_m &= -\lambda_{3,m}\mathbf{M}_{\mathbf{x},m}\mathbf{s}_m-\mathbf{C}_{\mathbf{x},m}\mathbf{s}_m+\mathbf{J}_m^{-T}\mathbf{Y}_{\mathbf{q},m}\tilde{\boldsymbol{\alpha}}_{\mathbf{q},m}\\ &+\mathbf{d}_{\mathbf{x},m}-\eta_m\,\mathrm{sgn}(\mathbf{s}_m)\end{aligned} \quad (21)$$

$$\mathbf{M}_{\mathbf{x},s}\dot{\mathbf{s}}_s = -\lambda_{3,s}\mathbf{M}_{\mathbf{x},s}\mathbf{s}_s - \mathbf{C}_{\mathbf{x},s}\mathbf{s}_s + \mathbf{J}_s^{-T}\mathbf{Y}_{\mathbf{q},s}\tilde{\boldsymbol{\alpha}}_{\mathbf{q},s} + \mathbf{M}_{\mathbf{x},s}k_{\mathrm{p}}\left(\hat{\ddot{\mathbf{x}}}_m^d - \ddot{\mathbf{x}}_m^d\right) + \mathbf{d}_{\mathbf{x},s} - \eta_s\,\mathrm{sgn}(\mathbf{s}_s) \quad (22)$$

3.4. Tracking Convergence Proof and Adaptation Laws

In order to prove the master and slave tracking convergence ($\mathbf{x}_m \to \mathbf{x}_{\mathrm{mod}_m}$, $\mathbf{x}_s \to \mathbf{x}_{\mathrm{mod}_s}$), a positive definite Lyapunov function candidate is proposed as

$$V(t) = \frac{1}{2}\left(\begin{array}{l}\mathbf{s}_m^T\mathbf{M}_{\mathbf{x},m}\mathbf{s}_m + \mathbf{s}_s^T\mathbf{M}_{\mathbf{x},s}\mathbf{s}_s \\ \qquad + \tilde{\boldsymbol{\alpha}}_{\mathbf{q},m}^T\boldsymbol{\Gamma}_m^{-1}\tilde{\boldsymbol{\alpha}}_{\mathbf{q},m} + \tilde{\boldsymbol{\alpha}}_{\mathbf{q},s}^T\boldsymbol{\Gamma}_s^{-1}\tilde{\boldsymbol{\alpha}}_{\mathbf{q},s}\end{array}\right) \quad (23)$$

where $\boldsymbol{\Gamma}_m$ and $\boldsymbol{\Gamma}_s$ are symmetric positive definite matrices. The time derivative of V is found by employing the final closed-loop dynamics (21) and (22), as

$$\begin{aligned}\dot{V}(t) &= -\lambda_{3,m}\mathbf{s}_m^T\mathbf{M}_{\mathbf{x},m}\mathbf{s}_m - \lambda_{3,s}\mathbf{s}_s^T\mathbf{M}_{\mathbf{x},s}\mathbf{s}_s \\ &+\frac{1}{2}\mathbf{s}_m^T\left(\dot{\mathbf{M}}_{\mathbf{x},m} - 2\mathbf{C}_{\mathbf{x},m}\right)\mathbf{s}_m + \frac{1}{2}\mathbf{s}_s^T\left(\dot{\mathbf{M}}_{\mathbf{x},s} - 2\mathbf{C}_{\mathbf{x},s}\right)\mathbf{s}_s \\ &+\mathbf{s}_m^T\mathbf{J}_m^{-T}\mathbf{Y}_{\mathbf{q},m}\tilde{\boldsymbol{\alpha}}_{\mathbf{q},m} + \mathbf{s}_m^T\left(\mathbf{d}_{\mathbf{x},m} - \eta_m\,\mathrm{sgn}(\mathbf{s}_m)\right) \\ &+\mathbf{s}_s^T\mathbf{J}_m^{-T}\mathbf{Y}_{\mathbf{q},s}\tilde{\boldsymbol{\alpha}}_{\mathbf{q},s} + \mathbf{s}_s^T\left(\mathbf{M}_{\mathbf{x},s}k_{\mathrm{p}}\left(\hat{\ddot{\mathbf{x}}}_m^d - \ddot{\mathbf{x}}_m^d\right)\right) \\ &+\mathbf{s}_s^T\left(\mathbf{d}_{\mathbf{x},s} - \eta_s\,\mathrm{sgn}(\mathbf{s}_s)\right) + \dot{\tilde{\boldsymbol{\alpha}}}_{\mathbf{q},m}^T\boldsymbol{\Gamma}_m^{-1}\tilde{\boldsymbol{\alpha}}_{\mathbf{q},m} + \dot{\tilde{\boldsymbol{\alpha}}}_{\mathbf{q},s}^T\boldsymbol{\Gamma}_s^{-1}\tilde{\boldsymbol{\alpha}}_{\mathbf{q},s}\end{aligned} \quad (24)$$

Now, the parameter adaptation laws are defined as

$$\dot{\tilde{\boldsymbol{\alpha}}}_{\mathbf{q},m} = -\boldsymbol{\Gamma}_m^T\,\mathbf{Y}_{\mathbf{q},m}^T\,\mathbf{J}_m^{-1}\,\mathbf{s}_m \;\;,\;\; \dot{\tilde{\boldsymbol{\alpha}}}_{\mathbf{q},s} = -\boldsymbol{\Gamma}_s^T\,\mathbf{Y}_{\mathbf{q},s}^T\,\mathbf{J}_s^{-1}\,\mathbf{s}_s \quad (25)$$

Then, using the above-mentioned adaptation laws (25) and Property 2 of robot dynamics, Eq. (24) simplifies to

$$\begin{aligned}\dot{V}(t) &= -\lambda_{3,m}\,\mathbf{s}_m^T\mathbf{M}_{\mathbf{x},m}\mathbf{s}_m - \lambda_{3,s}\,\mathbf{s}_s^T\mathbf{M}_{\mathbf{x},s}\mathbf{s}_s \\ &+\mathbf{s}_m^T\left(\mathbf{d}_{\mathbf{x},m} - \eta_m\,\mathrm{sgn}(\mathbf{s}_m)\right) \\ &+\mathbf{s}_s^T\left(\mathbf{M}_{\mathbf{x},s}k_{\mathrm{p}}\left(\hat{\ddot{\mathbf{x}}}_m^d - \ddot{\mathbf{x}}_m^d\right) + \mathbf{d}_{\mathbf{x},s} - \eta_s\,\mathrm{sgn}(\mathbf{s}_s)\right)\end{aligned} \quad (26)$$

In order to have robustness against the bounded disturbances and/or modeling mismatches ($\mathbf{d}_{\mathbf{x},m}$ and $\mathbf{d}_{\mathbf{x},s}$) and the bounded estimation error of the master robot acceleration ($\hat{\ddot{\mathbf{x}}}_m - \ddot{\mathbf{x}}_m$), the positive constant parameters η_m and η_s in the control laws (14) and (15) should satisfy the following inequalities:

$$\eta_m \geq \left\|\mathbf{d}_{\mathbf{x},m}\right\|_\infty + \mu_m \quad (27)$$

$$\eta_s \geq \left\|\mathbf{M}_{\mathbf{x},s}k_{\mathrm{p}}\left(\hat{\ddot{\mathbf{x}}}_m^d - \ddot{\mathbf{x}}_m^d\right)\right\|_\infty + \left\|\mathbf{d}_{\mathbf{x},s}\right\|_\infty + \mu_s \quad (28)$$

where μ_m and μ_s are positive constants. Note that the bounded error of the acceleration estimation ($\hat{\ddot{\mathbf{x}}}_m^d - \ddot{\mathbf{x}}_m^d$) is unknown. However, η_s should be chosen as large (using a practical trial and error method) that the stability of the system against bounded acceleration estimation error is ensured; which means the inequality (28) is satisfied. Then, the time derivative of Lyapunov function (26) can be written as

$$\dot{V}(t) \leq -\lambda_{3,m}\,\mathbf{s}_m^T\mathbf{M}_{\mathbf{x},m}\mathbf{s}_m - \lambda_{3,s}\,\mathbf{s}_s^T\mathbf{M}_{\mathbf{x},s}\mathbf{s}_s - \mu_m\left\|\mathbf{s}_m\right\|_1 - \mu_s\left\|\mathbf{s}_s\right\|_1 \quad (29)$$

The ∞-norm ($\|.\|_\infty$) and 1-norm ($\|.\|_1$) used in (27)-(29) are the vector norms obtained from the element values of each vector.

Theorem 1. The asymptotic convergence to sliding surfaces $\mathbf{s}_m = 0$ and $\mathbf{s}_s = 0$ is ensured using the proposed strategy.

Proof. Based on $V(t) > 0$ and $\dot{V}(t) \leq 0$, the Lyapunov function (23) is bounded, and consequently $\mathbf{s}_m$, $\mathbf{s}_s$, $\tilde{\boldsymbol{\alpha}}_{\mathbf{q},m}$ and $\tilde{\boldsymbol{\alpha}}_{\mathbf{q},s}$ are bounded. Then, the function $w(t) = \lambda_{3,m}\mathbf{s}_m^T\mathbf{M}_{\mathbf{x},m}\mathbf{s}_m + \lambda_{3,s}\mathbf{s}_s^T\mathbf{M}_{\mathbf{x},s}\mathbf{s}_s + \mu_m\left\|\mathbf{s}_m\right\|_1 + \mu_s\left\|\mathbf{s}_s\right\|_1 \geq 0$ is considered whose time derivative is $\dot{w}(t) = 2\lambda_{3,m}\mathbf{s}_m^T\mathbf{M}_{\mathbf{x},m}\dot{\mathbf{s}}_m + 2\lambda_{3,s}\mathbf{s}_s^T\mathbf{M}_{\mathbf{x},s}\dot{\mathbf{s}}_s + \lambda_{3,m}\mathbf{s}_m^T\dot{\mathbf{M}}_{\mathbf{x},m}\mathbf{s}_m + \lambda_{3,s}\mathbf{s}_s^T\dot{\mathbf{M}}_{\mathbf{x},s}\mathbf{s}_s + \mu_m\left(\mathrm{sgn}(\mathbf{s}_m).\dot{\mathbf{s}}_m\right) + \mu_s\left(\mathrm{sgn}(\mathbf{s}_s).\dot{\mathbf{s}}_s\right)$. With bounded non-singular inertia matrices $\mathbf{M}_{\mathbf{x},m}$ and $\mathbf{M}_{\mathbf{x},s}$, $\dot{\mathbf{s}}_m$ and $\dot{\mathbf{s}}_s$ are obtained as bounded vectors from Eqs. (21) and (22). Moreover, since the elements of $\mathbf{M}_{\mathbf{x},m}$ and $\mathbf{M}_{\mathbf{x},s}$ are in terms of differentiable functions, their time derivatives $\dot{\mathbf{M}}_{\mathbf{x},m}$ and $\dot{\mathbf{M}}_{\mathbf{x},s}$ are bounded. Based on the above-mentioned boundedness of matrices and vectors, $\dot{w}(t)$ is bounded; thus, $w(t)$ is uniformly continuous. Then, using (29), one can write:

$$V(0) - V(\infty) \geq \lim_{t\to\infty}\int_0^t w(\zeta)\,d\zeta \quad (30)$$

Based on (29), $\dot{V}(t) = dV(t)/dt \leq 0$ is negative, i.e., $V(0) - V(\infty) \geq 0$ is positive and finite. Thus, $\lim_{t\to\infty}\int_0^t w(\zeta)\,d\zeta$ in (30) exists and is finite and positive (due to the positiveness of $w(t)$). Therefore, according to the Barbalat's lemma [36]:

$$\lim_{t\to\infty} w(t) = \lim_{t\to\infty}\left(\lambda_{3,m}\mathbf{s}_m^T\mathbf{M}_{\mathbf{x},m}\mathbf{s}_m + \lambda_{3,s}\mathbf{s}_s^T\mathbf{M}_{\mathbf{x},s}\mathbf{s}_s + \mu_m\left\|\mathbf{s}_m\right\|_1 + \mu_s\left\|\mathbf{s}_s\right\|_1\right) = 0 \quad (31)$$

Since $\lambda_{3,m}$, $\lambda_{3,s}$, μ_m and μ_s are positive (nonzero) constants, $\mathbf{s}_m^T\mathbf{M}_{\mathbf{x},m}\mathbf{s}_m \geq 0$, $\mathbf{s}_s^T\mathbf{M}_{\mathbf{x},s}\mathbf{s}_s \geq 0$, $\left\|\mathbf{s}_m\right\|_1 \geq 0$ and $\left\|\mathbf{s}_s\right\|_1 \geq 0$, then Eq. (31) implies that the convergence to sliding surfaces $\mathbf{s}_m = 0$ and $\mathbf{s}_s = 0$ is achieved as $t \to \infty$.

Since the dynamics of the master and slave sliding surfaces $\mathbf{s}_m = 0$ and $\mathbf{s}_s = 0$ are stable (see Eq. (12)), the convergence of tracking errors to zero ($\tilde{\mathbf{x}}_m \to 0$ and $\tilde{\mathbf{x}}_s \to 0$) on the surfaces of $\mathbf{s}_m = 0$ and $\mathbf{s}_s = 0$ are proven.

4. Absolute Stability Proof

4.1. Llewellyn's Absolute Stability of the Teleoperation System

The absolute stability of a two-port network guarantees the stability of the coupled system connected to two passive but otherwise arbitrary one-port network terminations [35]. The relation between interaction forces and robots velocities of the two-port teleoperation system, in each direction (k) of space, is defined in terms of the so-called hybrid matrix ($\mathbf{H}_k$) as

$$\begin{bmatrix} F_{h,k}(s) \\ -V_{s,k}(s) \end{bmatrix} = \underbrace{\begin{bmatrix} h_{11,k} & h_{12,k} \\ h_{21,k} & h_{22,k} \end{bmatrix}}_{\mathbf{H}_k} \begin{bmatrix} V_{m,k}(s) \\ F_{e,k}(s) \end{bmatrix} \quad (32)$$

Theorem 2. The Llewellyn's stability criterion [38] introduces the sufficient conditions of the absolute stability as

(a) $h_{11,k}$ and $h_{22,k}$ do not have any pole in the right half of the complex plane (RHP).

(b) Any pole of $h_{11,k}$ and $h_{22,k}$ that is on the imaginary axis is simple with a real and positive residue.

(c) For all real values of ω ($s = j\omega$):

$$\begin{aligned} &\mathrm{Re}[h_{11,k}] \geq 0, \quad \mathrm{Re}[h_{22,k}] \geq 0, \\ &\eta(\omega) = 2\,\mathrm{Re}[h_{11,k}]\,\mathrm{Re}[h_{22,k}] - \mathrm{Re}[h_{12,k}h_{21,k}] - |h_{12,k}h_{21,k}| \geq 0 \end{aligned} \quad (33)$$

where η is called the stability margin value. Proof of this theorem is addressed in [35].

4.2. Resulted Hybrid Matrix and Stability Conditions

Since the master and slave sliding surfaces ($\mathbf{s}_m$ and $\mathbf{s}_s$ in (12)) are designed based on the impedance models (8) and (9), the closed-loop dynamics of robots are made asymptotically similar to the reference impedance models using the presented nonlinear BMRAIC scheme. Moreover, the initial positions of the master and slave robots as well as their initial velocities and accelerations are specified to be zero, the same as the master and slave reference impedance models' responses (i.e., $\mathbf{s}_m(0) = 0$ and $\mathbf{s}_s(0) = 0$ at $t = 0$). Also, if there is any non-zero oscillations, the convergence to sliding surfaces $\mathbf{s}_m \to 0$ and $\mathbf{s}_s \to 0$ are ensured as $t \to \infty$ (proof in Sec. 3.4), and tracking errors will converge to zero ($\tilde{\mathbf{x}}_m \to 0$ and $\tilde{\mathbf{x}}_s \to 0$).

As a result, the nonlinear teleoperation system will behave asymptotically similar to the two linear desired impedance models. Therefore, the hybrid matrix of the proposed teleoperation system in each Cartesian coordinate k is obtained from the realized reference impedance models (8) and (9) for the master and slave as

$$\begin{bmatrix} h_{11,k} & h_{12,k} \\ h_{21,k} & h_{22,k} \end{bmatrix} = \begin{bmatrix} m_m s + c_m & k_{\mathrm{f}}.\mathrm{e}^{-T_2 s} \\ -k_{\mathrm{p}}.\mathrm{e}^{-T_1 s} & \dfrac{s}{m_s s^2 + c_s s + k_s} \end{bmatrix} \quad (34)$$

Based on the above hybrid matrix (34) for the proposed teleoperation system, (a) and (b) conditions of the absolute stability criterion (Theorem 2) together with the first two conditions ($\mathrm{Re}[h_{11,k}] \geq 0$ and $\mathrm{Re}[h_{22,k}] \geq 0$) in (c) are satisfied by choosing positive impedance parameters. Using Eq. (34), the third condition in (c) for the stability margin value η is obtained as

$$\begin{aligned} \eta = &\frac{2c_m c_s \omega^2}{\left(k_s - m_s\omega^2\right)^2 + \left(c_s\omega\right)^2} \\ &+ k_{\mathrm{p}}k_{\mathrm{f}}\left[\cos\left(\left(T_1 + T_2\right)\omega\right) - 1\right] \geq 0 \end{aligned} \quad (35)$$

Therefore, if the positive impedance parameters of the master and slave robots satisfy the inequality (35) for the operating frequency range, the proposed teleoperation system is absolutely stable based on Theorem 2.

4.3. Notes on Absolute, Lyapunov and Asymptotic Stability for Teleoperation Systems

The Lyapunov stability for a controlled dynamic system means that the system response error (with respect to desired trajectory) can be kept arbitrarily close to zero by starting sufficiently close to it [36]. The asymptotic stability also means that the system trajectory error started close to zero actually converges to it as $t \to \infty$ [36]. Similarly, for teleoperation systems, the Lyapunov stability is used for the boundedness of both master and slave trajectory errors, and the Lyapunov asymptotic stability is employed for the convergence of these errors to zero. However, the absolute stability corresponds to the bounded behavior of the whole two-port teleoperation system and includes the input-to-output stability from each port to another port. As a result, the communication delays between master and slave robots affect the absolute stability conditions (as occurred in Sec. 4.2, Eq. (35)). On the other hand, the asymptotic convergence of master and slave trajectories to the delayed signals can be proved independently of the values of time delays (as expressed in Sec. 3.4).

Note that the master trajectory signal ($\mathbf{x}_m$ in Figs. 1 and 2) is sent to the slave robot and the interaction force signal from the slave site ($\mathbf{f}_e$ in Figs. 1 and 2) is fed back to the master robot using the proposed bilateral controller. Accordingly, the behaviour of the slave robot may become undesirable due to the tracking of master signal $\mathbf{x}_m^d$ with bounded delay. This results in undesirable behaviour of the master robot due to the employment of delayed signal $\mathbf{f}_e^d$ from the slave robot in the master controller. Consequently, without the absolute stability, responses of both master and slave robots may become undesirable or unstable due to the communication delays; however, the convergence of tracking errors (Laypunov asymptotic stability) is proved in Sec. 3.4. Thus, the absolute stability is required to be analyzed for delayed two-port teleoperation systems as well as the Lyapunov asymptotic stability. In other words, the asymptotic stability only guarantees the convergence of master and slave tracking errors to zero, not the bounded behavior of the whole bilateral system. Therefore, the absolute stability is very essential in systems with multi ports that influence each other.

5. The Procedure of Choosing Impedance parameters

5.1. Step 1. Position and Force Scaling Factors

The position and force scaling factors (k_{p} and k_{f} in (9) and (8)) may be chosen based on the workspace size ratio of the robots and the desired scaling of the environment force feedback provided to the human operator.

5.2. Step 2. Impedance Parameters of Master

Parameters m_m and c_m of the master reference impedance model (8) should be chosen sufficiently small such that the desired force tracking performance ($\mathbf{f}_h \to k_{\mathrm{f}}\,\mathbf{f}_e^d$) is approximately achieved (this was discussed in Sec. 3.1).

5.3. Step 3. Impedance Parameters of Slave

The reference impedance model (9) of the slave robot in each direction (k) of the Cartesian coordinates can be presented in the Laplace form as $s^2 + 2\zeta_s\omega_{n_s}s + \omega_{n_s}^2$, where $\zeta_s = c_s \big/ 2\sqrt{m_s k_s}$ and $\omega_{n_s} = \sqrt{k_s/m_s}$ are the damping ratio and natural frequency of this model, respectively. In order to have a fast response (with respect to the dimensionless time $\omega_{n_s} t$) and minimum overshoot value (in response to the step force), the damping ratio is chosen as $\zeta_s \simeq 0.7$. The settling time, $t_{s_s} = 3\big/(\zeta_s\omega_{n_s})$, for 5% tolerance criterion can be adjusted. The stiffness k_s of slave impedance model (9) is adjusted on a large value such that the slave robot has an acceptable small deviation ($\tilde{\mathbf{x}}_{\mathrm{mod}_s}$), as discussed in Sec. 3.1. Using the specified values of ζ_s , t_{s_s} and k_s , the mass m_s and damping c_s parameters are also determined.

5.4. Step 4. Modification of Parameters for Absolute Stability

In this step, the chosen parameters for the master and slave impedance models in previous steps are revised to guarantee the absolute stability (Theorem 2) in the presence of communication delays. This is done by satisfying inequality (35) in the range of working frequency. For this purpose, the partial derivatives of $\eta(\omega)$ in (35) with respect to the parameters of the impedance models are determined. Then, the frequency intervals in which the decrease of each impedance parameter will increase $\eta(\omega)$ (i.e. $\partial\eta\big/\partial z_i < 0$) and enhance the stability of the teleoperation system are obtained and presented in Table 1.

This table will help the designer to increase the value of stability margin $\eta(\omega)$ by decreasing and/or increasing the parameters (k_{p} , k_{f} , c_m , c_s , m_s and k_s) until inequality (35) is satisfied in different frequency intervals.

Note that the position and force tracking performances may be undermined by modification of the impedance parameters to guarantee the absolute stability. Accordingly, a trade-off between the transparency (position and force tracking) and the absolute stability is needed in the presence of time delays.

Table 1 The frequency intervals in which $\partial\eta(\omega)\big/\partial z_i < 0$

Parameter z_i	Frequency Interval
k_{p} , k_{f}	All frequencies
c_m	No frequency ($\partial\eta\big/\partial c_m$ is positive for all frequencies)
c_s	$\dfrac{-c_s + \sqrt{c_s^2 + 4k_s m_s}}{2m_s} < \omega < \dfrac{c_s + \sqrt{c_s^2 + 4k_s m_s}}{2m_s}$
m_s	$\omega > \sqrt{k_s/m_s} = \omega_{n_s}$
k_s	$0 < \omega < \sqrt{k_s/m_s} = \omega_{n_s}$

6. Experimental Results

In this section, the proposed controller is evaluated by some experiments on a three-DOF Phantom Premium 1.5A robot (Geomagic Inc., Wilmington, MA) and a two-DOF Quanser planar robot (Quanser Consulting Inc., Markham, ON) shown in Fig. 3 as the master and slave robots with nonlinear dynamics, respectively. The Phantom Premium and Quanser robots are respectively equipped with a 6-axis JR3 50M31 force/torque sensor (JR3 Inc., Woodland, CA) and a 6-axis ATI Gamma force/torque sensor (ATI Industrial Automation, Apex, NC). Both of the master (Phantom) and the slave (Quanser) robots can move in the $x-y$ plane as shown in Fig. 3. The third Cartesian DOF of the Phantom robot in z (vertical) direction is controlled at zero position. The kinematics and dynamics of the Phantom and Quanser robots were presented in [39] and [40], respectively.

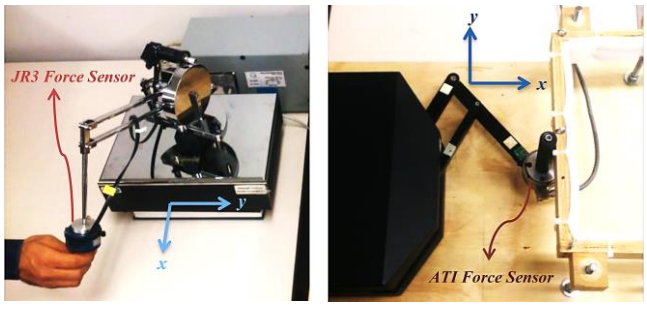

Fig. 3. *The experimental setup: Phantom Premium robot (left) and Quanser robot (right) as the master and slave robots, respectively.*

6.1. Case 1: Delay-Free Communication Channels

In the case of delay-free communication channels, the values of impedance parameters and scaling factors are chosen based on Steps 1-3 of Sec. 5, as listed in Table 2.

Table 2 Master and slave impedance parameters, and scaling factors for delay free communication channels ($T_1 = T_2 = 0$)

Master impedance parameters	Slave impedance parameters	Position and force scaling factors
$m_m = 0.1$ kg	$m_s = 9.80$ kg	$k_p = 1$
$c_m = 0.3$ N.s/m	$c_s = 293.98$ N.s/m	$k_f = 1/3$
	$k_s = 4500$ N/m	

As it is observed in Fig. 4a, the interaction forces ($\mathbf{f}_h$ and $k_f\mathbf{f}_e$) are very close to one another, which is the result of choosing small master impedance parameters m_m and c_m (in Table 2). However, due to the sudden changes of hard (wooden) environment force $\mathbf{f}_e$ at the beginning and the end of interaction, the force tracking error ($\mathbf{f}_h - k_f\mathbf{f}_e$) has some jumps (less than 0.6 N) at these moments as shown in Fig. 4b.

Figure 5 demonstrates the position responses and errors of robots with respect to their reference impedance models. According to Fig. 5, the position tracking performance (between the master and slave) is achieved in the teleoperation system. This performance is the result of a) choosing large values for the slave impedance parameters (i.e. large m_s , c_s and k_s result in small $\tilde{\mathbf{x}}_{\text{mod}_s}$) as discussed in Sec. 3.1, and b) tracking error convergence of the master and slave trajectories ($\tilde{\mathbf{x}}_m \to 0$ and $\tilde{\mathbf{x}}_s \to 0$) using the proposed bilateral controller that was proven in Sec. 3.4.

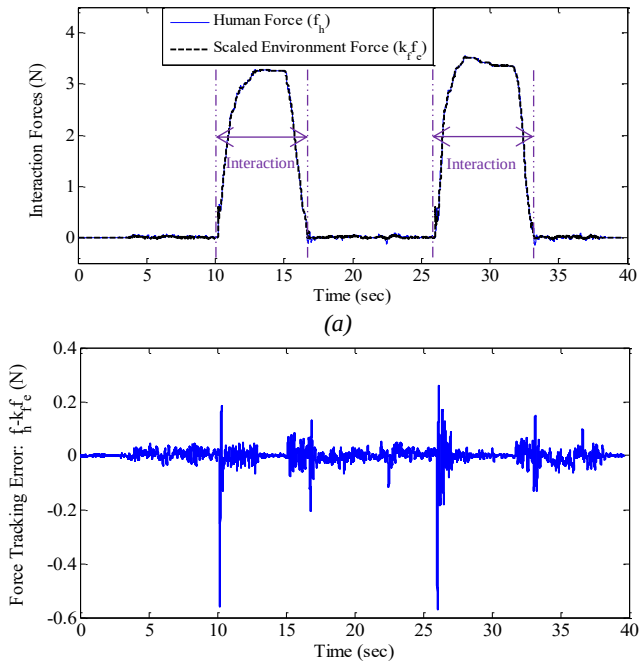

Fig. 4. *(a) Interaction forces with (b) their difference in x direction.*

As the results show, in the absence of communication delays ($T_1 = T_2 = 0$), the transparency conditions (position and force tracking) are realized with small errors.

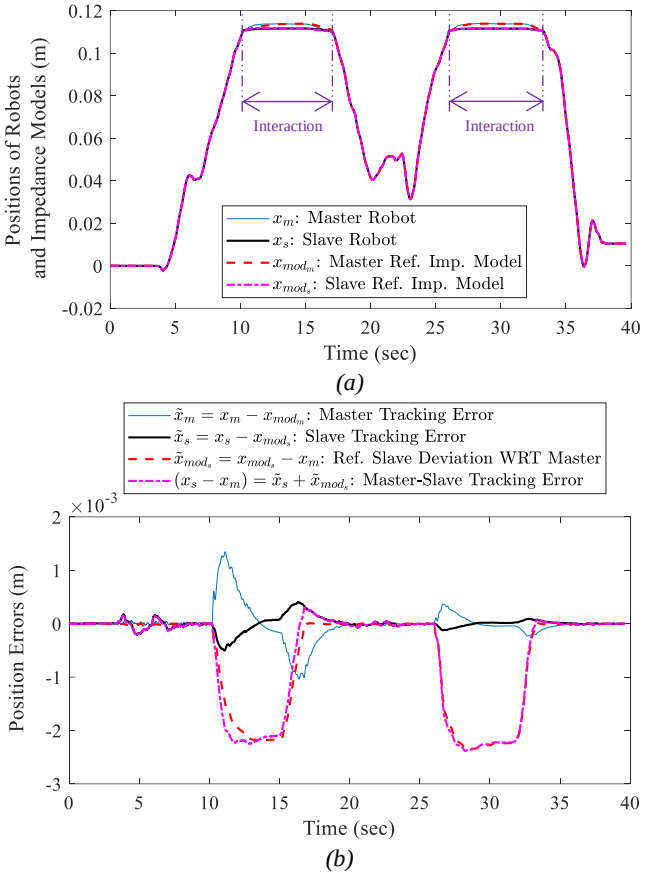

Fig. 5. *(a) Positions of the master and slave robots together with their reference models responses, and (b) position tracking errors, in x direction.*

6.2. Case 2: Delayed Communication Channels

In this section, the proposed bilateral controller is evaluated experimentally in the presence of constant time delays in the communication channels ($T_1 = 50$ *msec* and $T_2 = 50$ *msec*). In this case, the arbitrary impedance parameters (listed in Table 2 for delay-free case) are modified based on Step 4 of Sec. 5 to guarantee the stability criterion (35). These modified values of impedance parameters are presented in Table 3.

Table 3 The modified impedance parameters, and scaling factors for delayed communication channels ($T_1 = 50$ *msec* and $T_2 = 50$ *msec*)

Master impedance parameters	Slave impedance parameters	Position and force scaling factors
$m_m = 0.1$ kg	$m_s = 0.001$ kg	$k_p = 1$
$c_m = 10.8$ N.s/m	$c_s = 20.5$ N.s/m	$k_f = 1/3$
	$k_s = 450$ N/m	

In this case, as illustrated in Fig. 6a, the position error of the slave with respect to the master is larger than the case of no delay. This is a consequence of the reduction to the slave impedance parameters (k_s , c_s and m_s) due to the stability requirements (explained in Sec. 5.4).

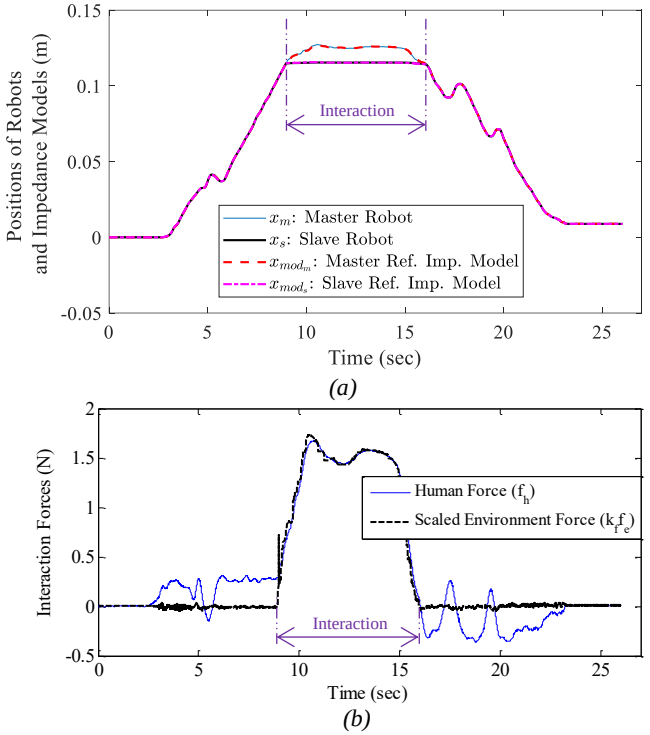

Fig. 6. *(a) Position of master and slave robots with their reference models responses and (b) the interaction forces* $\mathbf{f}_h$ *and* $k_f\mathbf{f}_e$ *, in* x *direction for delayed communication channels and using modified impedance parameters.*

Figure 6b shows that the interaction forces ($\mathbf{f}_h$ and $k_f\mathbf{f}_e$) closely match each other during the interaction, when the robots' velocities are near zero. However, before and after the interaction when the robots have non-zero velocities and accelerations and the slave robot moves in free space ($\mathbf{f}_e \approx 0$), the applied human force $\mathbf{f}_h$ is not near zero. This performance occurs as a result of the modification and increase of the master impedance parameter c_m based on Step 4 of Sec. 5 to ensure the absolute stability in the presence of time delays.

7. Concluding Remarks

A new nonlinear Bilateral Model Reference Adaptive Impedance Controller (BMRAIC) was developed for nonlinear multi-DOF teleoperation systems. The controller employs the parameters of stable reference impedance models in its structure to make the closed-loop dynamics of the master and slave robots similar to their reference models. The proposed bilateral controller realizes the impedance models in the presence of parametric and bounded unstructured modeling (non-parametric) uncertainties as it was proven using the Lyapunov theorem.

The absolute stability of the nonlinear multi-DOF teleoperation system is guaranteed in the presence of communication delays by adjusting the desired impedance parameters. As a result, using the presented bilateral impedance controller and the corresponding stability analysis, a trade-off between the stability and transparency of the teleoperation system is provided when communication channels have time delays. The presented experiments on multi-DOF nonlinear master and slave robots show the performance of the proposed bilateral controller and its stability in hard tissue interactions with and without communication delays.

8. References

[1] Tavakoli, M., Aziminejad, A., Patel, R.V., and Moallem, M., 'Methods and Mechanisms for Contact Feedback in a Robot-Assisted Minimally Invasive Environment', *Surgical Endoscopy And Other Interventional Techniques*, 2006, 20, (10), pp. 1570-1579.

[2] Takhmar, A., Polushin, I.G., Talasaz, A., and Patel, R.V., 'Cooperative Teleoperation with Projection-Based Force Reflection for Mis', *IEEE Transactions on Control Systems Technology*, 2015, 23, (4), pp. 1411-1426.

[3] Carignan, C.R. and Krebs, H.I., 'Telerehabilitation Robotics: Bright Lights, Big Future?', *Journal of Rehabilitation Research and Development*, 2006, 43, (5), pp. 695-710.

[4] Shahbazi, M., Atashzar, S.F., Tavakoli, M., and Patel, R.V., 'Robotics-Assisted Mirror Rehabilitation Therapy: A Therapist-in-the-Loop Assist-as-Needed Architecture', *IEEE/ASME Transactions on Mechatronics*, 2016, 21, (4), pp. 1954-1965.

[5] Najafi, F. and Sepehri, N., 'Design and Prototyping of a Force-Reflecting Hand-Controller for Ultrasound Imaging', *Journal of Mechanisms and Robotics*, 2011, 3, (2), p. 021002 (11 pages).

[6] Colgate, J.E., 'Robust Impedance Shaping Telemanipulation', *Robotics and Automation, IEEE Transactions on*, 1993, 9, (4), pp. 374-384.

[7] Dongjun, L. and Li, P.Y., 'Passive Bilateral Feedforward Control of Linear Dynamically Similar Teleoperated Manipulators', *Robotics and Automation, IEEE Transactions on*, 2003, 19, (3), pp. 443-456.

[8] Chen, Z., Pan, Y.J., and Gu, J., 'Adaptive Robust Control of Bilateral Teleoperation Systems with Unmeasurable Environmental Force and Arbitrary Time Delays', *IET Control Theory & Applications*, 2014, 8, (15), pp. 1456-1464.

[9] Polushin, I.G., Liu, P.X., Lung, C.-H., and On, G.D., 'Position-Error Based Schemes for Bilateral Teleoperation with Time Delay: Theory and Experiments', *Journal of Dynamic Systems, Measurement, and Control*, 2010, 132, (3), p. 031008 (11 pages).

[10] Li, J.N. and Li, L.S., 'Reliable Control for Bilateral Teleoperation Systems with Actuator Faults Using Fuzzy Disturbance Observer', *IET Control Theory & Applications*, 2017, 11, (3), pp. 446-455.

[11] Wen-Hong, Z. and Salcudean, S.E., 'Stability Guaranteed Teleoperation: An Adaptive Motion/Force Control Approach', *Automatic Control, IEEE Transactions on*, 2000, 45, (11), pp. 1951-1969.

[12] Malysz, P. and Sirouspour, S., 'Nonlinear and Filtered Force/Position Mappings in Bilateral Teleoperation with Application to Enhanced Stiffness Discrimination', *Robotics, IEEE Transactions on*, 2009, 25, (5), pp. 1134-1149.

[13] Lee, D. and Spong, M.W., 'Passive Bilateral Teleoperation with Constant Time Delay', *Robotics, IEEE Transactions on*, 2006, 22, (2), pp. 269-281.
[14] Nuño, E., Ortega, R., and Basañez, L., 'An Adaptive Controller for Nonlinear Teleoperators', *Automatica*, 2010, 46, (1), pp. 155-159.
[15] Liu, Y.C. and Chopra, N., 'Control of Semi-Autonomous Teleoperation System with Time Delays', *Automatica*, 2013, 49, (6), pp. 1553-1565.
[16] Kang, Y., Li, Z., Shang, W., and Xi, H., 'Motion Synchronisation of Bilateral Teleoperation Systems with Mode-Dependent Time-Varying Communication Delays', *IET Control Theory & Applications*, 2010, 4, (10), pp. 2129-2140.
[17] Ryu, J.H. and Kwon, D.S., 'A Novel Adaptive Bilateral Control Scheme Using Similar Closed-Loop Dynamic Characteristics of Master/Slave Manipulators', *Journal of Robotic Systems*, 2001, 18, (9), pp. 533-543.
[18] Liu, X. and Tavakoli, M., 'Adaptive Control of Teleoperation Systems with Linearly and Nonlinearly Parameterized Dynamic Uncertainties', *Journal of Dynamic Systems, Measurement, and Control*, 2012, 134, (2), p. 021015 (10 pages).
[19] Mohammadi, A., Tavakoli, M., and Marquez, H.J., 'Disturbance Observer-Based Control of Non-Linear Haptic Teleoperation Systems', *IET Control Theory & Applications*, 2011, 5, (18), pp. 2063-2074.
[20] Hashemzadeh, F., Sharifi, M., and Tavakoli, M., 'Nonlinear Trilateral Teleoperation Stability Analysis Subjected to Time-Varying Delays', *Control Engineering Practice*, 2016, 56, pp. 123-135.
[21] Sun, D., Naghdy, F., and Du, H., 'Wave-Variable-Based Passivity Control of Four-Channel Nonlinear Bilateral Teleoperation System under Time Delays', *IEEE/ASME Transactions on Mechatronics*, 2016, 21, (1), pp. 238-253.
[22] Sun, D., Naghdy, F., and Du, H., 'A Novel Approach for Stability and Transparency Control of Nonlinear Bilateral Teleoperation System with Time Delays', *Control Engineering Practice*, 2016, 47, pp. 15-27.
[23] Yang, C., Wang, X., Li, Z., Li, Y., and Su, C.Y., 'Teleoperation Control Based on Combination of Wave Variable and Neural Networks', *IEEE Transactions on Systems, Man, and Cybernetics: Systems*, 2017, 47, (8), pp. 2125-2136.
[24] Yang, Y., Hua, C., and Guan, X., 'Finite Time Control Design for Bilateral Teleoperation System with Position Synchronization Error Constrained', *IEEE Transactions on Cybernetics*, 2016, 46, (3), pp. 609-619.
[25] Martínez, C.A.L., Molengraft, R.v.d., Weiland, S., and Steinbuch, M., 'Switching Robust Control for Bilateral Teleoperation', *IEEE Transactions on Control Systems Technology*, 2016, 24, (1), pp. 172-188.
[26] Chen, Z., Pan, Y.-J., and Gu, J., 'Integrated Adaptive Robust Control for Multilateral Teleoperation Systems under Arbitrary Time Delays', *International Journal of Robust and Nonlinear Control*, 2016, 26, (12), pp. 2708-2728.
[27] Hogan, N., 'Impedance Control: An Approach to Manipulation: Part I---Theory', *Journal of Dynamic Systems, Measurement, and Control*, 1985, 107, (1), pp. 1-7.
[28] Sharifi, M., Behzadipour, S., and Vossoughi, G.R., 'Model Reference Adaptive Impedance Control of Rehabilitation Robots in Operational Space', in, *Biomedical Robotics and Biomechatronics (BioRob), 4th IEEE RAS & EMBS International Conference on*, (2012).
[29] Abdossalami, A. and Sirouspour, S., 'Adaptive Control for Improved Transparency in Haptic Simulations', *Haptics, IEEE Transactions on*, 2009, 2, (1), pp. 2-14.
[30] Sharifi, M., Behzadipour, S., and Vossoughi, G., 'Nonlinear Model Reference Adaptive Impedance Control for Human–Robot Interactions', *Control Engineering Practice*, 2014, 32, pp. 9-27.
[31] Hashtrudi-Zaad, K. and Salcudean, S.E., 'Analysis of Control Architectures for Teleoperation Systems with Impedance/Admittance Master and Slave Manipulators', *The International Journal of Robotics Research*, 2001, 20, (6), pp. 419-445.
[32] Cho, H.C. and Park, J.H., 'Stable Bilateral Teleoperation under a Time Delay Using a Robust Impedance Control', *Mechatronics*, 2005, 15, (5), pp. 611-625.
[33] Abbott, J.J. and Okamura, A.M., 'Pseudo-Admittance Bilateral Telemanipulation with Guidance Virtual Fixtures', *The International Journal of Robotics Research*, 2007, 26, (8), pp. 865-884.
[34] Liu, X., Tao, R., and Tavakoli, M., 'Adaptive Control of Uncertain Nonlinear Teleoperation Systems', *Mechatronics*, 2014, 24, (1), pp. 66-78.
[35] Haykin, S.S., *Active Network Theory*, (Addison-Wesley Pub. Co., 1970).
[36] Slotine, J.J.E. and Li, W., *Applied Nonlinear Control*, (Prantice-Hall, 1991).
[37] Sharifi, M., Behzadipour, S., and Vossoughi, G.R., 'Model Reference Adaptive Impedance Control in Cartesian Coordinates for Physical Human–Robot Interaction', *Advanced Robotics*, 2014, 28, (19), pp. 1277-1290.
[38] Haddadi, A. and Hashtrudi-Zaad, K., 'Bounded-Impedance Absolute Stability of Bilateral Teleoperation Control Systems', *Haptics, IEEE Transactions on*, 2010, 3, (1), pp. 15-27.
[39] Çavuşoğlu, M.C., Feygin, D., and Tendick, F., 'A Critical Study of the Mechanical and Electrical Properties of the Phantom Haptic Interface and Improvements for High-Performance Control', *Presence: Teleoperators & Virtual Environments*, 2002, 11, (6), pp. 555-568.
[40] Dyck, M.D., 'Measuring the Dynamic Impedance of the Human Arm', M.Sc. Thesis, University of Alberta, 2013.